Journal of Photopolymer Science and Technology
Volume 27, Number 5 (2014) 611–615 © 2014SPST

Electron Penetration Depths in EUV Photoresists

Justin Torok,[a] Bharath Srivats,[a] Shahid Memon,[a] Henry Herbol,[a] Jonathan Schad,[a] Sanjana Das,[a] Leonidas Ocola,[b] Greg Denbeaux[a] and Robert L. Brainard[a]

a. College of Nanoscale Science and Engineering, University at Albany
257 Fuller Rd. Albany NY 12203
b. Argonne National Laboratories, Cass Ave. Argonne IL 60439

One of the obstacles hindering the transition from 193 nm to extreme ultraviolet (EUV) photolithography is photoresist performance. However, design of next generation chemically-amplified EUV resists necessitates that we fully understand the mechanisms underlying photoacid generation. In particular, we would like to determine the effective distance the low-energy electrons generated during EUV exposure travel within resists while continuing to induce photoacid generator (PAG) decomposition, since diffusion length carries important implications for resolution and line edge roughness. Here, we demonstrate two novel experimental approaches for obtaining electron diffusion length in resists using top-down electron beam exposure: thickness loss experiments and in situ mass spectrometry.

Key Words: EUV, Secondary Electrons, Penetration Depth, Photoresist

1. Introduction

The continued demand for increasing transistor density in semiconductor manufacturing requires that the resolution of photolithography also improves. Historically, this industry has transitioned to lower wavelengths of light every eight to ten years to shrink the minimum printable feature size. As 193-nm lithography reaches its resolution limit, the leading candidate to replace it for future nodes is extreme ultraviolet (EUV, $\lambda = 13.5$ nm) lithography. One of the most significant factors preventing EUV from entering mainstream production, however, is the need for new photoresists that can utilize the lower wavelength of light for higher resolution without compromising sensitivity and line edge roughness. A central design consideration is that EUV photons interact with matter in a manner entirely different from the higher-wavelength photons traditionally used in semiconductor manufacturing. While 193-nm light has only enough energy to promote an electron in a photoacid generator (PAG) chromophore from a bonding orbital to an antibonding orbital [1,2], EUV radiation has enough energy (92 eV per photon) to ionize molecules within the resist. In the latter case, it is the cascade of events following primary photoelectron generation that induces PAG decomposition and catalytic acid production; therefore, in order to understand how to best design EUV photoresists, we need to study how low-energy electrons (0-80 eV) propagate within polymer films and interact with molecules within the resist.

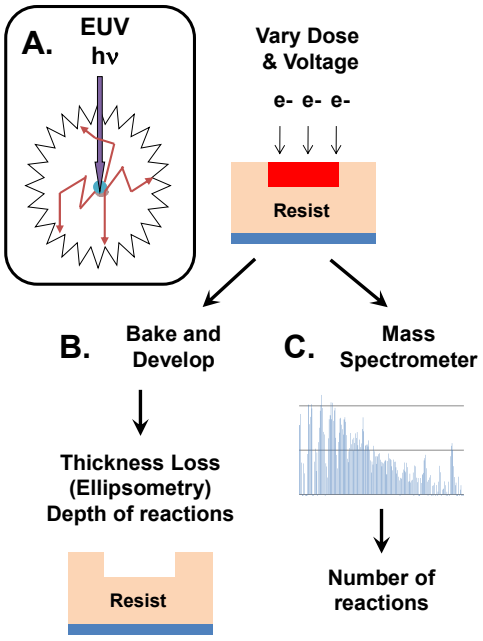

Figure 1. (A) Schematic of secondary electron diffusion from the EUV photon absorption site. (B)

Received April 24, 2014
Accepted May 30, 2014

Process flow of our (B) thickness loss experiments and (C) mass-spectrometer experiments to determine depth of electron travel.

Previous work conducted by our group addressed the potential mechanisms behind acid generation during EUV exposure from a theoretical perspective [3]. In this work, we explore the diffusion lengths of various energies using top-down electron beam exposures of different EUV resists. Determining the effective distance low-energy electrons travel from the initial EUV photon absorption site and cause chemistry is critical to understanding how the latent image is formed during EUV exposure, which carries important implications for resolution and LER. We can directly study electron interactions with EUV resists using top-down electron beam exposures and a combination of thickness loss experiments and mass spectrometry (Figure 1). The thickness loss as a result of e-beam exposure is a reflection of the penetration depth of reactive electrons, allowing us to determine the effective diffusion length of electrons of a given energy and glean information about the distribution of PAG decomposition reactions with respect to depth. We also use *in situ* mass spectrometry to more directly examine the chemical transformations within the photoresist during e-beam exposure. Conventional EUV photoacid generators, such as onium sulfonates, decompose to form volatile byproducts that escape from the resist film under vacuum; we can therefore track acid generation in real time by measuring the outgassing of the resist at specific atomic masses. Though our outgassing results are preliminary at this time, our initial findings demonstrate that mass spectrometry holds promise as a tool for studying electron-PAG interactions.

2. Experimental

2.1 Thickness-Loss Experiments

We exposed a 60 nm commercial resist film using a Kimball electron gun in a custom-built vacuum chamber. After processing under manufacturer-specified conditions, we measured the change in thickness using an ellipsometer.

2.2 Mass-Spectrometry Experiments

We used a 60 nm open source resist film (See Figure 4 for exact composition) and measured the outgassing signal during e-beam exposure using an Extrel mass spectrometer.

3. Results and Discussion

3.1Thickness Loss Experiments

The results of our thickness loss experiments are displayed in Figure 2. We chose four representative electron energies (50, 100, 500 and 1000 eV) and exposed the resist at doses spanning over four orders of magnitude. The maximum thickness loss observed was greatest for 1000 eV electrons (which cleared the entire thickness of the film) and decreased commensurately for lower energies. The higher energies also required a lower dose to clear a given resist thickness. For example, 100 eV electrons require 10 $\mu C/cm^2$ to remove 10 nm of resist, whereas 500 eV electrons require less than 1 $\mu C/cm^2$ to remove 10 nm. It is tempting to conclude that electrons of each energy have a maximum penetration depth from Figure 2A, as the thickness loss *vs.* dose profiles of the lower energies appear to plateau. However, when viewed on a logarithmic scale (Figure 2B), the profiles are approximately linear, suggesting that further increases in dose will continue to induce chemistry deeper into the resist. Because the process of electron penetration through a resist film is ultimately a stochastic process, there is always a small but finite probability that low energy electrons may travel arbitrarily long distances before interacting with a PAG molecules. Thus, even though it may be extremely unlikely for a 50 eV electron to react with a PAG molecule 10 nm from the surface of the resist film, for example, at exceedingly high doses, enough acids are generated at that depth to switch the resist from insoluble to soluble in developer. If the dose ranges were extended beyond 150 $\mu C/cm^2$, we expect that we would continue to see increases in thickness loss at all energies.

Though we cannot yet determine the precise penetration depth of electrons of a specific energy, we can use the data shown in Figure 2 to infer an approximate distribution of the locations of PAG reactions during exposure. Suppose that

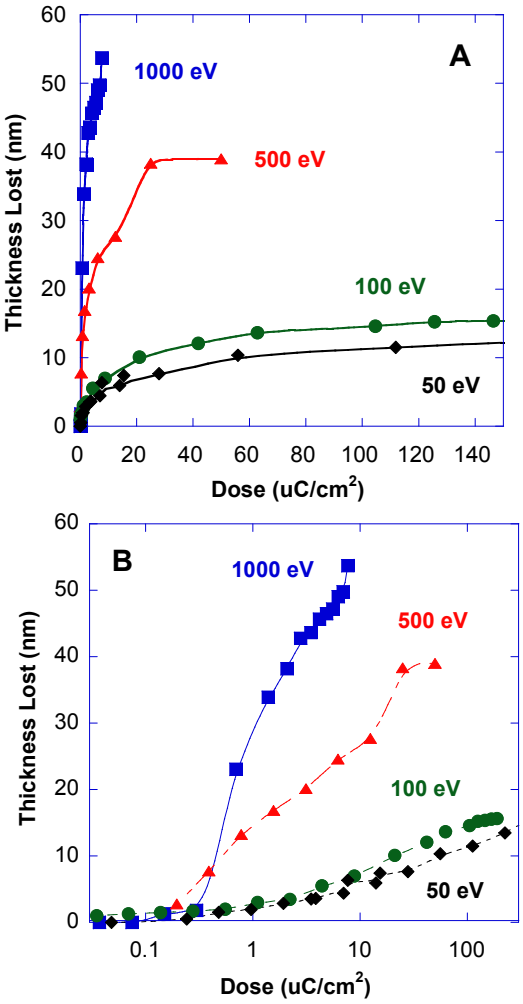

Figure 2. Thickness loss in nm plotted against dose at four different energies, both on a linear scale (A) and a log scale (B).

exposure by electrons of a certain energy clears 10 nm of resist at 10 μC/cm^2 and 15 nm of resist at 20 μC/cm^2. In the latter case, an additional 10 μC/cm^2 was required to remove 5 nm beyond the first 10 nm. Therefore, half as many reactions occur in the region of resist 10-15 nm below the surface than in the top 10 nm during exposure.

Extending this logic, we can then replot the data in Figure 2 in terms of the number of relevant reactions (in arbitrary units) *versus* depth in the resist and obtain a distribution of acid generation events for each energy (Figure 3). These reaction profiles do not necessarily reflect distribution of electron ranges during exposure, but from them we can estimate the depth at which the large majority of electrons cease to cause reactions. However, the actual number of reactions occurring during exposure at a specific depth is dose-dependent. For example, even though a small fraction of the total number of reactions 1000 eV electrons cause are at a depth of 50 nm or greater, at high enough doses, enough reactions occur in this region to dissolve the resist to this depth.

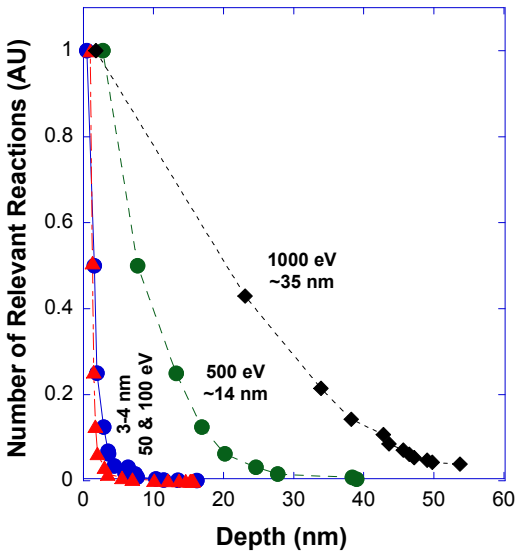

Figure 3. Relevant reactions in arbitrary units *vs.* depth at which reactions are occurring; data is identical to those in Figure 2 but are replotted as described in the text. We can approximate from this graph an effective reaction depth at which most of the reactions are occurring during exposure for each energy.

3.2 Mass Spectrometry Studies

For quanti-tative information about photoacid generator decomposition during exposure, we expose an open source resist, herein referred to as OS4 (Figure 4), and observe the production of volatile PAG byproducts with mass spectrometry. A representative spectrum obtained from OS4 is shown in Figure 5. There are two prominent peaks corresponding to decomposition products of the triphenyl-sulfonium perfluorobutanesulfonate PAG: one at mass 78 (benzene) and another at mass 186 (diphenyl sulfide). For the following experiments, we focused exclusively on benzene outgassing.

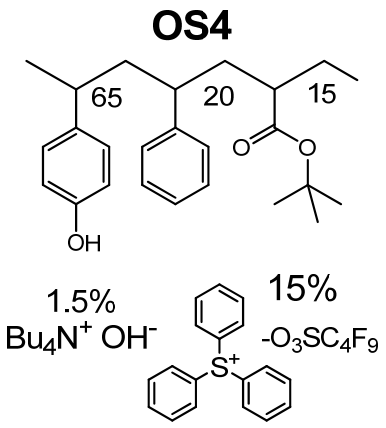

Figure 4. Composition of the open source resist (OS4) used for our mass spectrometry experiments.

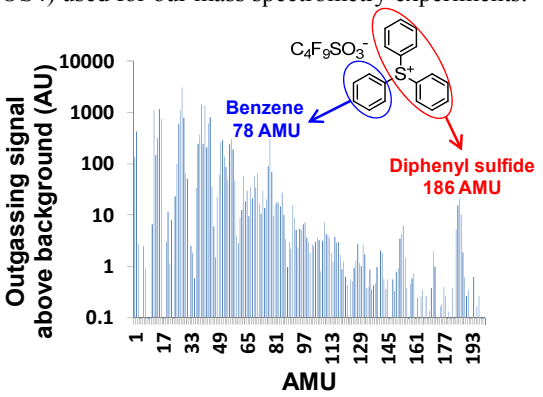

Figure 5. Representative mass spectrum of OS4 spanning masses 1-200 amu. The two peaks corresponding to PAG decomposition products are located at masses 78 and 186, which correspond to benzene and diphenyl sulfide, respectively.

One potential pitfall of mass spectrometry is that it requires the decomposition products to leave the film; if the resist is only slightly permeable to the molecule under observation, then it is possible that there is a depth below which no reactions can be detected. To determine if diffusion was a limiting factor to our analysis, we performed short, one-second exposures at several energies, waiting sufficiently long between exposures to allow the benzene signal to fully attenuate (Figure 6). Since higher energy electrons cause chemistry deeper within the resist than lower energy electrons and the time scale of outgassing signal decay is related to benzene diffusion, the signal attenuation should occur more slowly at higher energies. However, if the film is not freely permeable, then we would expect the decay rate to be constant for all energies that induce PAG decomposition beyond the maximum escape depth of benzene. After fitting each curve with an exponential so that we could quantitatively compare signal attenuation rates between exposures, we found that the decay time increased with energy. Notably, the time constant for 2000 eV electrons was three times larger than the time constant for 700 eV electrons, suggesting that a significant fraction of the benzene outgassing at 2000 eV is from PAG decomposition in the bottom half of the resist. Simulations performed by our group predict that 700 eV electrons are reactive through the top 30 nm of resist while 2000 eV electrons generate acid throughout the full 60 nm (data not shown).

To confirm that mass spectrometry is capable of following PAG decomposition in real time, we continuously irradiated a 1 cm^2 sample of OS4 with 2000 eV electrons until we observed benzene outgassing return to baseline (Figure 7). The dose required to saturate the outgassing response was many times the E_0 of OS4 at this energy (1.3 $\mu C/cm^2$), indicating that the full thickness of the film will clear after only a small fraction of the total PAG molecules present have decomposed. We also found that the attenuation of the outgassing signal was very closely exponential in shape, suggesting that PAG decomposition displays first-order kinetics; in other words, the rate of decomposition of PAG is proportional to the PAG concentration in the film.

4. Conclusions

We have developed two complementary methods to study electron propagation through photoresist films: thickness loss experiments and PAG decomposition monitoring using mass spectrometry. Our thickness loss measurements give us a means to quantitate how far in the resist electrons of various energies are able to travel and still induce chemistry, which also

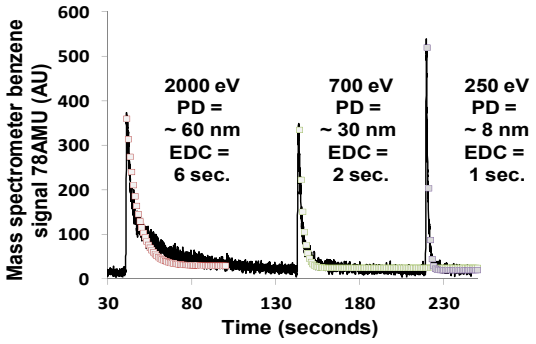

Figure 6. Outgassing at 78 amu for one-second exposures at various energies. The black line is the raw output of the mass spectrometer in counts; the gray points are the exponential fits determined for the 2000, 700, and 250 eV exposures, respectively. PD = Penetration Depth; EDC = Exponential Decay Constant

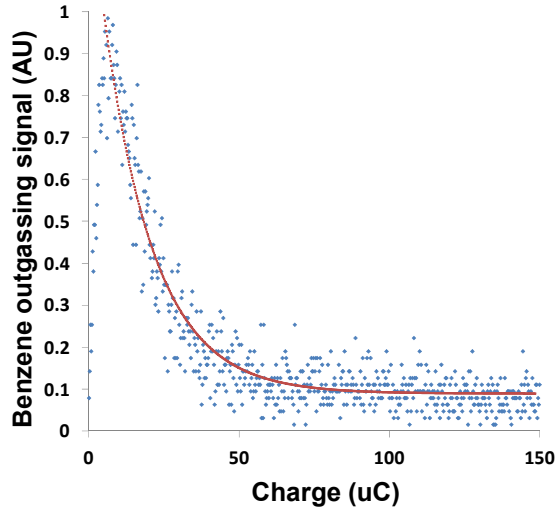

Figure 7. Continuous exposure to saturation at 2000 eV. The y-axis is the outgassing signal normalized to the peak value observed during exposure and the x-axis is the cumulative dose in μC applied during exposure. The blue data points are the raw outgassing data; the red line is the calculated exponential fit.

allows us to determine the distribution of acid generation events during exposure. On the other hand, *in situ* mass spectrometry can be used to track PAG decomposition in real time, from which we can extract not only the penetration depth of reactive electrons but also information about the kinetics of the acid generation reaction. We are currently refining our methodology so that we can extend our experiments to lower energies more relevant to EUV. Ultimately, we believe these experiments will shed considerable insight into the nature of secondary electron-resist interactions, which in turn will allow us to design more efficient, higher performance EUV photoresists.

5. Acknowledgements

We thank the College of Nanoscale Science and Engineering (CNSE) and specifically, Senior Vice President Alain Kaloyeros for financial support of this project. We also thank the supplier of our commercial resist. The use of the Center for Nanoscale Materials, Argonne National Laboratory was supported by the U.S. Department of Energy, Office of Science, Office of Basic Energy Sciences, under Contract No. DE-AC02-06CH11357.

References

[1] R. Brainard, G. Barclay, E. Anderson and L. Ocola, *Microelectronic Engineering*. **61–62** (2002) 707–715.

[2] Y. Wei and R. Brainard, Advanced Processes for 193-nm Immersion Lithography, SPIE Press, Bellingham, WA, 2009.

[3] J. Torok, R. Del Re, H. Herbol, S. Das, I. Bocharova, A. Paolucci, L. E. Ocola, C. Ventrice, Jr., E. Lifshin, G. Denbeaux and R. Brainard, *J. Photopolym. Sci. Technol.*, **26** (2013) 625-634

.